JOURNAL OF NEUROTRAUMA 37:1–10 (XXXX XX, 2020)

DOI: 10.1089/neu.2020.7086

Original Article

Continuous Optical Monitoring of Spinal Cord Oxygenation and Hemodynamics during the First Seven Days Post-Injury in a Porcine Model of Acute Spinal Cord Injury

Amanda Cheung,[1] Lorna Tu,[1] Neda Manouchehri,[1] Kyoung-Tae Kim,[1,2] Kitty So,[1] Megan Webster,[1] Shera Fisk,[1] Seth Tigchelaar,[1] Sara S. Dalkilic,[1] Eric C. Sayre,[3] Femke Streijger,[1] Andrew Macnab,[4] Brian K. Kwon,[1,5,*] and Babak Shadgan[1,5,*]

Abstract

One of the only currently available treatment options to potentially improve neurological recovery after acute spinal cord injury (SCI) is augmentation of mean arterial blood pressure (MAP) to promote blood flow and oxygen delivery to the injured cord. However, to optimize such hemodynamic management, clinicians require a method to monitor the physiological effects of these MAP alterations within the injured cord. Therefore, we investigated the feasibility and effectiveness of using a novel optical sensor, based on near-infrared spectroscopy (NIRS), to monitor real-time spinal cord oxygenation and hemodynamics during the first 7 days post-injury in a porcine model of acute SCI. Six Yucatan miniature pigs underwent a T10 vertebral level contusion-compression injury. Spinal cord oxygenation and hemodynamics were continuously monitored by a minimally invasive custom-made NIRS sensor, and by invasive intraparenchymal (IP) probes to validate the NIRS measures. Episodes of MAP alteration and hypoxia were performed acutely after injury, and at 2 and 7 days post-injury to simulate the types of hemodynamic changes SCI patients experience after injury. The NIRS sensor demonstrated the ability to provide oxygenation and hemodynamic measurements over the 7-day post-SCI period. NIRS measures showed statistically significant correlations with each of the invasive IP measures and MAP changes during episodes of MAP alteration and hypoxia throughout the first week post-injury ($p < 0.05$). These results indicate that this novel NIRS system can monitor real-time changes in spinal cord oxygenation and hemodynamics over the first 7 days post-injury, and has the ability to detect local tissue changes that are reflective of systemic hemodynamic changes.

Keywords: animal model; hemodynamics; implantable sensor; near-infrared spectroscopy; spinal cord injury

Introduction

Neurological damage from acute traumatic spinal cord injury (SCI) occurs in two stages: the primary injury caused by the immediate trauma and the secondary injury that results from the pathophysiological responses that follow the primary trauma.[1,2] It is during this acute injury phase that clinicians are able to take advantage of attenuating these pathophysiological responses to prevent further damage. Although much attention has been paid to novel drug therapies for acute SCI,[3,4] two treatment approaches are commonly used in clinical practice in an attempt to improve neurological outcome: 1) urgent surgical decompression and 2) aggressive hemodynamic management.[5–7] Both options aim to improve blood flow and oxygen delivery to the injured spinal cord tissue.

The importance of hemodynamic management and its potential to improve neurological recovery has been considered for years.[8–11] The current clinical guidelines for the treatment of acute SCI recommend that mean arterial blood pressure (MAP) be augmented to 85–90 mm Hg for 7 days post-injury.[7] However, the evidence that links specific MAP targets to improved neurological outcome is surprisingly weak.[12–14] One of the reasons why it may be difficult to demonstrate that specific MAP targets improve neurological outcome is that clinicians are unable to determine how

[1]International Collaboration on Repair Discoveries, [4]Department of Pediatrics, [5]Department of Orthopedics, University of British Columbia, Vancouver, British Columbia, Canada.
[2]Department of Neurosurgery, School of Medicine, Kyungpook National University, Kyungpook National University Hospital, Daegu, South Korea.
[3]Arthritis Research Canada, Richmond, British Columbia, Canada.
*These authors contributed equally.

changes in MAP affect blood flow and oxygen delivery within the injury site to mitigate ischemia and cellular death. There is currently no method to monitor the real-time response of these spinal cord physiological measures to alterations in MAP over the first 7 days post-injury.[15] Having a method to continuously monitor spinal cord oxygenation and hemodynamics would help clinicians optimize hemodynamic management, and enable them to more comprehensively evaluate the effects of this intervention on neurological outcome. To address this need, we developed a sensor, based on near-infrared spectroscopy (NIRS), that could monitor real-time spinal cord oxygenation and hemodynamics in a minimally invasive manner.[16]

NIRS is a well-established optical technology clinically used to monitor oxygen delivery in various tissues such as the brain and skeletal muscle.[17–20] It is a non-invasive (non-destructive) method that uses near-infrared (NIR) light (700–1000 nm) to monitor regional tissue oxygenation and hemodynamics.[21] Photons in the NIR spectrum are transmitted into the tissue where the chromophores, oxygenated hemoglobin (O_2Hb) and deoxygenated hemoglobin (HHb), absorb NIR light in a wavelength-dependent manner.[22,23] O_2Hb and HHb have an equal absorption spectra at 800 nm, whereas at 760 nm, NIR light has a peak absorption by HHb.[24] By using a single multi-wavelength (MW) light source and one photodetector, NIRS has the capacity to monitor changes in tissue oxygen delivery, consumption, and utilization as measured by O_2Hb and HHb concentrations and the oxygenated-deoxygenated hemoglobin difference (Hbdiff = O_2Hb – HHb), a relative measure of tissue oxygenation.[25–28] Changes in total hemoglobin (THb = O_2Hb + HHb) reflect local blood volume, an index of local microcirculatory hemodynamics.[29,30] Using spatially resolved (SR) or MW configurations to measure changes in light attenuation between multiple light sources and photodetectors, NIRS can also provide an absolute quantitative measure of tissue oxygenation by calculating the tissue oxygenation index (TOI).[16,31,32]

We previously investigated a customized NIRS sensor for real-time monitoring of spinal cord oxygenation in a porcine model of acute SCI.[16] In fully anesthetized pigs, we demonstrated a high degree of sensitivity and specificity of NIRS-derived O_2Hb, Hbdiff, and TOI in detecting spinal cord oxygenation changes during the first 5–6 h post-injury.[16] Acknowledging that patients with acute SCI currently have MAP augmentation for up to 7 days and are not always fully anesthetized during this period, we sought to extend our evaluation of the NIRS sensor into a more clinically relevant setting. Hence, in this study, we designed a new NIRS sensor and investigated its ability to continuously monitor spinal cord oxygenation and hemodynamic changes for 7 days post-injury in a porcine model of acute SCI, even in awake, mobile animals.

Methods

All animal protocols and procedures performed in this study were approved by the Animal Care Committee of the University of British Columbia (UBC) and were compliant with the policies of the Canadian Council of Animal Care and the U.S. Army Medical Research and Materiel Command (USAMRMC) Animal Care and Use Review Office (ACURO). The anesthesia/analgesia protocols were established by the UBC Center for Comparative Medicine.

Customized NIRS sensor

The customized miniature NIRS sensor that we developed for this study (Fig. 1) was a modification of the sensor applied in our first study.[16] The current sensor (Pathonix Innovation Inc., Vancouver, BC, Canada) consists of a single MW light-emitting diode (LED) capable of emitting NIR light in five wavelengths (660, 730, 810, 850, and 950 nm) with a total output power of 2 mW (Shenzhen Keborui Electronics Co., Ltd., Shenzhen, China) and one small silicon photodetector. The inter-optode distance is 10 mm to enable light penetration of a depth of 5 mm. The sensor has a width of 5 mm and is encased inside a durable, fluid-resistant, and transparent medical-grade catheter. Our goal in designing this new sensor was to make it similar in size to a surgical drain used routinely after human surgeries to evacuate blood from the epidural space. This allowed the sensor to be externalized percutaneously through the skin away from the surgical wound and then pulled out in its entirety at the end of the 7-day period. The sensor was connected to the NIRS controller unit by a flexible, multi-branch, shielded wire to protect against potential electromagnetic interference.

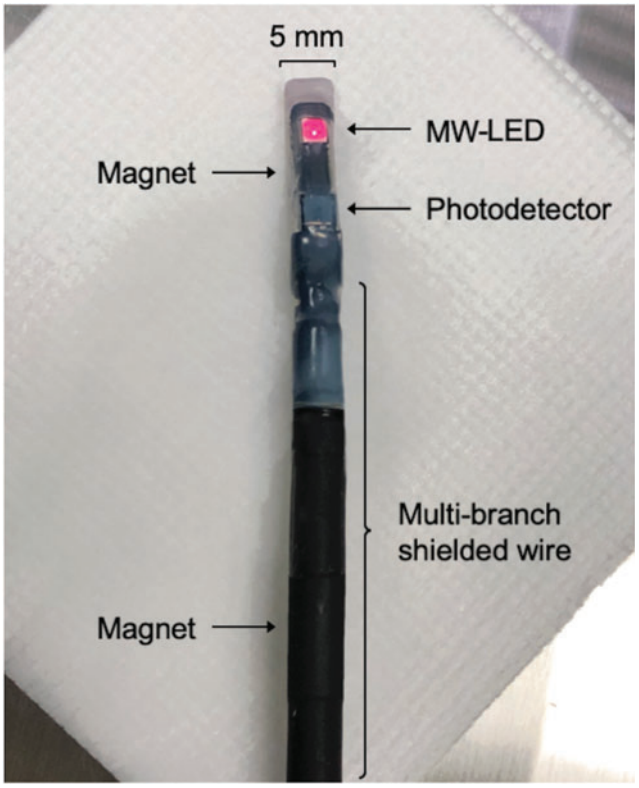

FIG. 1. Customized implantable NIRS sensor. The NIRS sensor consists of one single multi-wavelength light-emitting diode (MW-LED) with 5 NIR wavelengths and one silicon photodetector. The NIRS sensor is connected to the NIRS controller unit by a multi-branch shielded wire, and magnets (on the other side of the sensor) are used to stabilize the sensor over the dura. LED, light-emitting diode; MW, multi-wavelength; NIRS, near-infrared spectroscopy. Color image is available online.

Sensor fixation system

To stabilize the NIRS sensor optode over the dura for 7-day data collection in a survival porcine model of SCI, a fixation system was designed. This fixator provided three degrees of freedom for fine adjustment of the sensor's optode. A small magnetic component (N52; K&J Magnetics Inc., Pipersville, PA, USA) was mounted at the fixator's arm to stabilize the sensor's optode over the dura (Fig. 2B). The wire of the NIRS sensor was sutured to the skin of

the animal at the entry site to prevent unnecessary movement of the sensor inside the animal and the sutures were then removed at the end of the 7-day monitoring period. This mode of magnetic fixation to secure the sensor on top of the dura in a ''non-rigid'' fashion allowed for the sensor to be pulled out at the end of the week of monitoring, avoiding an additional surgery to retrieve the sensor.

Sensor operating system

We utilized an upgraded version of our previously developed customized MW-NIRS controller unit with microchip firmware that controlled the sensor's NIR light emission and processed all the relayed information on emission, absorption, scatter, and detection of each NIR wavelength (Fig. 2C).[16] The controller unit transmitted this information through a standard USB-C cable to a dedicated laptop computer running a customized NIRS software. The system used a mathematical algorithm derived from a modified Beer-Lambert Law to process the light attenuation of each wavelength related to the absorption of O_2Hb and HHb, and then translate this information to the relative concentrations of these chromophores.

The software also calculated TOI using an additional algorithm we developed to analyze the light attenuation of the five wavelengths. Our calculation of TOI in porcine spinal cord tissue was validated in our previous study, in which a statistically significant correlation between TOI and blood-gas-derived capillary oxygen saturation percentage ($S_{cap}O_2$) was found.[16] The controller unit and operating software were upgraded to support long-term, 7-day data collection. The upgraded software also included the ability to adjust the intensity and gain of each wavelength separately during data collection to fine-tune the emitter. This feature allowed better adjustment of light emission and detection to enable higher consistency across animals. The NIRS signals were collected and recorded at 100 Hz and the software graphically displayed O_2Hb, HHb, THb, Hbdiff, and TOI in real time.

Porcine model of SCI

Six female Yucatan miniature pigs weighing between 25 and 31 kg at the time of surgery were used in this study. Animals were prepared for surgery, and intubated and anesthetized as previously described.[33,34] A pulse oximeter was attached to the animal's ear to monitor arterial oxygen saturation (SaO_2) levels and heart rate at a frequency of 0.25 Hz. The right left carotid artery and jugular vein were exposed by blunt dissection. The carotid artery was catheterized (18 Gauge Arterial Catheterization Set FA-04018; Arrow International, Reading, PA, USA) to monitor invasive MAP at a frequency of 10 Hz. The jugular vein was catheterized (7 French Multi-Lumen Central Venous Catheterization Set CE-12703; Arrow International) to perform norepinephrine (NE) and nitroprusside (NP) infusions to deliberately increase and decrease the MAP, respectively. The animal was then carefully repositioned into a prone position. A dorsal laminectomy was performed between vertebral levels T5 and L1 to expose the dura and underlying spinal cord, and the T10 vertebral level was identified and marked as the intended impact site.

The T5, T9, T10, T11, and T14 vertebrae were instrumented bilaterally with pedicle screws (3.5×25 mm Vertex screws; Medtronic, Memphis, TN, USA) and titanium rods. An articulating arm (660 Magnetic Base Indicator Holder; Starrett, Athol, MA, USA) was attached to this construct for proper positioning of the impact device, which consisted of an impactor (diameter of 0.953 cm) fitted with a load cell (LLB215; Futek Advanced Sensor Technology, Irvine, CA, USA) to record the force at impact. The impactor slid down a guide rail equipped with a Balluff Micropulse® linear position sensor (BTL6-G500-M0102-PF-S115; Balluff Canada Inc., Mississauga, ON, Canada) to record the impactor position, from which displacement and velocity were determined.

Five minutes prior to the contusion-compression SCI, a single intravenous fentanyl bolus was administered to achieve effective pain relief during the impact. The contusion was induced by dropping the 50 g impactor along the guide rail onto the cord at the vertebral T10 level from a height of 16.73 cm. An additional 100 g mass was gently added for a total compression weight of 150 g. After 30 min of sustained compression, the cord was decompressed by removing the additional mass and impactor.

Intraparenchymal probes and NIRS sensor placement

Before SCI, two sets of two intraparenchymal (IP) probes were inserted into the spinal cord and the NIRS sensor was positioned on the spinal cord (Fig. 2). In each set of IP probes, one probe was used for dual monitoring of spinal cord blood flow (SCBF), which employed laser Doppler flowmetry,[35] and the partial pressure of oxygen (PO_2), which used a fluorescence quenching and fiber-optic technology (0.45 mm diameter; NX-BF/OF/E; Oxford Optronix, Abingdon, UK).[36] The second IP probe was used for monitoring spinal cord pressure (SCP; 0.31 mm diameter; FOP-LS-NS-1006A; FISO Technologies Inc., Harvard Apparatus, Saint-Laurent, QC, Canada), which used a fiber-optic combined Fabry-Perot interferometry pressure sensor.[37,38] SCBF and PO_2 were recorded at a sampling rate of 10 Hz and SCP was recorded at a sampling rate of 1 Hz. The IP probes were inserted through the skin and into catheters, which were placed into a custom three dimensional (3-D) printed housing unit with precision-drilled holes to guide probe insertion and secure the probes in place.[39,40] The IP probes were then inserted through the dura into the spinal cord at a 45-degree angle, with the tips situated at a depth of approximately 3–4 mm under the dura, 1.5 cm and 3.5 cm caudal from the center of the intended impact site. Ultrasound imaging (L14-5/38, 38 mm linear array probe, Ultrasonix RP; BK Ultrasound, Richmond, BC, Canada) was performed to verify proper probe placement inside the spinal cord and determine the actual probe tip position.

The NIRS sensor was tunneled through the skin using a Hemovac surgical trocar (Fig. 2A). The sensor was positioned on top of the dura 3.5 cm rostral from the center of the intended T10 injury site and held in place using lateral connectors and magnet-based fixators. This was as close to the injury site as the sensor could be placed to ensure it would not be affected by the actual impact. Fibrin bio-adhesive sealant (Tisseel®; Baxter Healthcare, Deerfield, IL, USA) was applied to the area around the sensor to further maintain gentle contact with the cord and to prevent blood from seeping under the sensor, potentially interfering with photon transmission. The wires from the IP probes and NIRS sensor were percutaneously brought out of the surgical field.

Experimental protocol

On the first day of the experiment (Day 1), the IP probes and NIRS sensor were positioned and the physiological parameters of interest were allowed to stabilize before continuous monitoring began. Baseline monitoring occurred for 60 min, followed by a series of events or ''physiological challenges'' as shown in the experimental timeline (Fig. 3). Two mild hypoxic episodes were induced by detaching the ventilator from the pig. It was reattached when oxygen saturation, as indicated by the pulse oximeter, reached 80%. Each hypoxic episode lasted for approximately 30 sec. The pig was then allowed to recover for 15 min. After the contusion-compression SCI and 30 min after decompression, MAP was increased by 20 mm Hg by infusing NE via the jugular vein

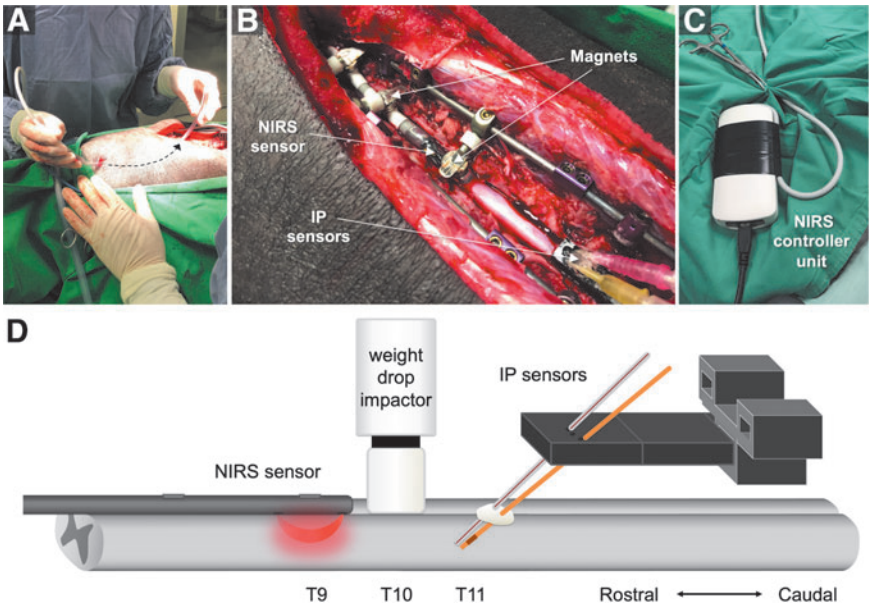

FIG. 2. NIRS sensor application. **(A)** A surgical trocar is used to tunnel the NIRS sensor through the skin and into the surgical wound. **(B)** The NIRS sensor is placed and fixed on the dura at vertebral level T9 using rods and magnetic fixators. Invasive IP probes are inserted in the spinal cord at vertebral level T11. **(C)** The NIRS sensor is connected to the NIRS controller unit and the wire is externalized, allowing the entire sensor to be pulled out at the end of the monitoring period without a second surgery to retrieve it. **(D)** Schematic of the IP probes and NIRS sensor placement. IP, intraparenchymal; NIRS, near-infrared spectroscopy. Color image is available online.

catheter. The target MAP was maintained for 30 min and the average NE dose was 0.33 ± 0.07 (range 0.11–0.64) μg/kg/min. The incision was then closed, and the sensors remained internalized to continuously collect data over 7 days. The externalized recording wires were attached to a suspended beam with a counterbalance lever system positioned above the center of the animal pen.[33] The lever system with counterweights kept the sensor wires away from the animal's reach, preventing tangling and damage of the sensor wires, while also allowing the pig to recover and move freely inside its enclosure. Post-operative recovery was managed as previously described.[33]

On the second day post-injury (Day 3), MAP alterations were performed on the awake, non-sedated pig. NE was infused intravenously to increase MAP by 20 mm Hg and the average NE dose was 0.42 ± 0.02 (range 0.37–0.46) μg/kg/min. After the target MAP was reached and maintained for 30 min, infusion of NE ended, and the animal was allowed to recover for 30 min. MAP was then decreased by 20 mm Hg using NP. The target MAP was maintained for 30 min and the average NP dose was 0.27 ± 0.06 (range 0.07–0.43) μg/kg/min.

On the seventh day post-injury (Day 8), the pig was sedated, intubated, and anesthetized. MAP alterations were performed in a similar manner as on previous days, but with MAP targets maintained for 60 min instead of 30 min. Each MAP alteration was followed by a 30-min recovery period. The average NE dose was 0.46 ± 0.09 (range 0.17–0.74) μg/kg/min and the average NP dose was 0.43 ± 0.12 (range 0.08–0.75) μg/kg/min. After increasing and decreasing the MAP, two severe hypoxic episodes were induced until the oxygen saturation reached 70%. Each episode lasted for about 45 sec, followed by 15 min of recovery time. The pig was then euthanized. After 5 min, we stopped recording data from the NIRS sensor and IP probes. The entire NIRS sensor was pulled out through its original percutaneous insertion site (similar to the clinical removal of a surgical drain) and IP probes were surgically removed.

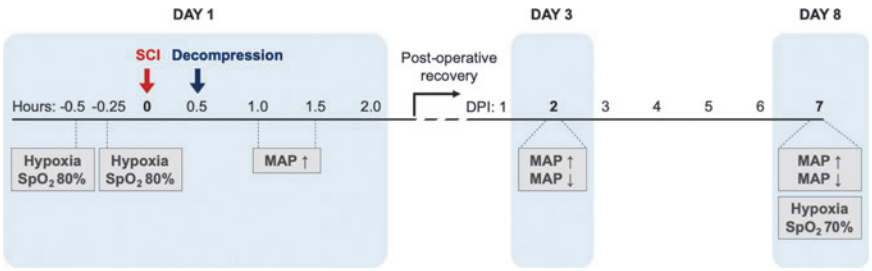

FIG. 3. Experimental protocol. Following baseline measurements on the day of surgery (Day 1), two episodes of mild hypoxia (oxygen saturation [SpO_2] 80%), T10 vertebral level contusion SCI, 30 min of sustained compression, cord decompression, and one 30-min episode of MAP increase were performed. On 2 days post-injury (Day 3), one 30-min episode each of MAP increase and decrease were performed. On 7 days post-injury (Day 8), one 60-min episode each of MAP increase and decrease, and two episodes of severe hypoxia (SpO_2 70%) were performed. MAP, mean arterial blood pressure; SCI, spinal cord injury. Color image is available online.

Statistical analysis

NIRS measures of spinal cord chromophore concentrations (O_2Hb and HHb), spinal cord IP measures (SCBF, PO_2, and SCP), and vital signs (SaO_2, heart rate, and respiratory rate) were continuously recorded throughout the 7-day experiment. Before MAP alterations were performed, baseline MAP levels were determined by the average MAP calculated from the most recent 15 min of MAP recordings. The raw optical data were converted into changes in NIRS parameters (O_2Hb and HHb), and THb, Hbdiff, and TOI were calculated via the NIRS software. Movement artifacts were observed when the animals were awake and mobile in their cages, which resulted in clear and distinguishable artifacts that were identified, marked, and removed from the data manually. The changes for each variable during each event, including spinal cord NIRS-derived O_2Hb, HHb, THb, Hbdiff, TOI, and IP-measured PO_2 and SCBF were compared with 0 using the Wilcoxon signed-rank test to determine statistical significance. Pearson correlation coefficients were calculated to establish the pairwise relationships between the NIRS and IP measurements during episodes of induced hypoxia and during the pharmacological increases and decreases in MAP. Bland-Altman plot analyses were used to evaluate the agreement between NIRS and IP measurements.[41,42] Data are presented as mean ± standard error of the mean (SEM) and the level of significance was set at $p < 0.05$ for all statistical analysis and comparisons. Data were analyzed using SAS version 9.4 (SAS Institute, Cary, NC, USA) and GraphPad Prism 8.3.0 (GraphPad Software, La Jolla, CA, USA).

Results

Six female Yucatan pigs with a mean weight of 27.5 ± 0.89 kg were studied. The customized miniature NIRS sensor successfully monitored spinal cord oxygenation and hemodynamics (O_2Hb, HHb, Hbdiff, TOI, and THb) during experimental interventions in all animals. One animal with a pre-existing respiratory and cardiac condition experienced complications. No health complications resulted from placement of the NIRS sensor and continuous monitoring. At the end of the 7-day experiment, we were able to easily pull the entire NIRS sensor and cable out through the surgical incision site.

Spinal cord injury biomechanics

We measured the impact force and subsequently calculated impulse, displacement, and velocity to evaluate the consistency of the injury between animals ($n = 6$). The average impact force applied to the exposed spinal cord was 4023.36 ± 144.18 kdyn (mean ± SEM) with an impulse of 12.80 ± 0.38 kdyn*sec. The average displacement of the impactor from initial contact with the exposed dura was 4.58 ± 0.27 mm with a velocity of 1970.81 ± 7.75 mm/sec at impact. Individual impact biomechanics for each animal are presented in Table 1.

IP versus NIRS parameters

To compare the minimally invasive NIRS measurements with the invasive IP measurements, we continuously measured both parameters during physiological manipulations from the day of surgery (Day 1) to 7 days post-injury (Day 8; Fig. 3). NIRS measurements were collected approximately 3.5 cm rostral to the injury site. For a similar comparison of measurements from the same distance away from the epicenter of injury, we used the IP data collected by the probes placed 3.5 cm caudal to the injury site. Hypoxia induction pre-SCI on Day 1 resulted in a sudden drop in PO_2 measured with the IP catheter, which was also observed in the NIRS oxygenation parameters of Hbdiff and O_2Hb (Fig. 4). This response was also captured on Day 8 in the same animal.

In addition, increasing MAP by NE infusion 30 min after decompression on Day 1 resulted in an increase in the IP measure of SCBF and a similar increase in the NIRS measure of THb. This response was maintained on Day 8 in the same animal (Fig. 5). Overall, the ability of the NIRS sensor to monitor spinal cord oxygenation and hemodynamic changes during hypoxic events and MAP alterations on the day of surgery (Day 1) was maintained 7 days post-injury (Day 8), demonstrating that the NIRS sensor can maintain meaningful physiological measurements over the 7-day post-SCI period.

Relationship between IP and NIRS measures and MAP

Analysis of the continuous 7-day data collected minimally invasively via the NIRS sensor and invasively via the IP probes demonstrated statistically significant correlations between the NIRS and IP measures of oxygenation and hemodynamics, particularly during the experimentally induced physiological challenges of hypoxia and MAP alterations (Table 2). Importantly, the NIRS measures of O_2Hb, Hbdiff, and TOI were strongly associated with the invasive IP measure of PO_2, and NIRS-measured THb was strongly related to IP-measured SCBF during the physiological challenges. The NIRS measures of O_2Hb, TOI, Hbdiff, and THb also demonstrated statistically significant correlations to changes in MAP during the induced increases and decreases in MAP.

Bland-Altman plots displayed agreement between NIRS O_2Hb and Hbdiff with IP PO_2. Analysis of the relationship between O_2Hb and PO_2 revealed a mean difference of 1.158 with upper and lower

Table 1. Measures of Weight and Injury Parameters

Animal #	*Body weight (kg)*	*Force (kdynes)*	*Impulse (kdynes*sec)*	*Displacement (mm)*	*Impact velocity (mm/sec)*
1	31.0	4548.20	12.11	4.47	1978.58
2	29.0	3595.44	12.83	4.36	1988.35
3	26.0	3758.58	11.77	3.91	1973.54
4	25.0	4270.77	12.39	4.47	1988.69
5	27.5	3859.88	14.27	5.84	1952.86
6	26.5	4107.31	13.44	4.46	1942.84
Mean	27.5	4023.36	12.80	4.58	1970.81
SEM	0.89	144.18	0.38	0.27	7.75

Body weight, force, impulse, displacement, and velocity measurements at impact are shown for each animal. Data are presented as mean ± SEM.
SEM, standard error of the mean.

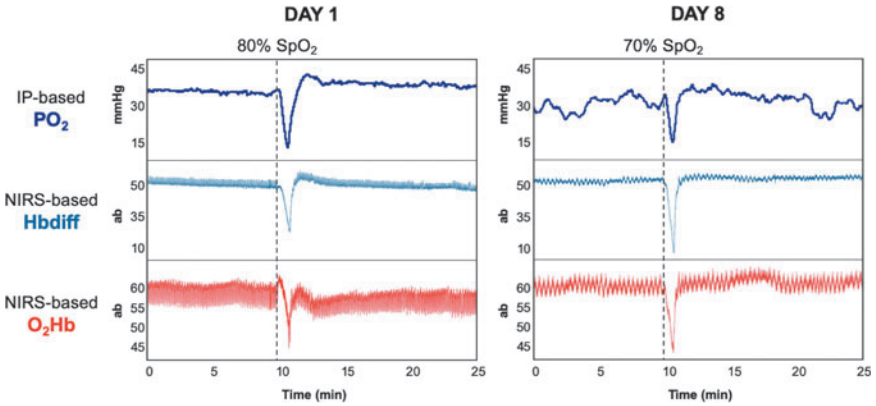

FIG. 4. Hypoxic challenge. On Day 1, hypoxia results in a significant drop in PO_2 measured with the IP sensor, which is also visualized in the chromophore concentration (ab) of NIRS-derived O_2Hb and the Hbdiff waveform. Similar responses are observed on Day 8 in the same animal. Hbdiff, oxygenated-deoxygenated hemoglobin difference; IP, intraparenchymal; NIRS, near-infrared spectroscopy; O_2Hb, oxygenated hemoglobin; PO_2, partial pressure of oxygen. Color image is available online.

limits of agreement of −28.27 and 30.59, respectively (Fig. 6A). Hbdiff and PO_2 ($n=6$) demonstrated a mean difference of −8.647 with upper and lower limits of agreement of −56.53 and 39.24 (Fig. 6B). The majority of the differences between the NIRS measures of O_2Hb and Hbdiff compared with IP PO_2 were within the limits of agreement, demonstrating that both O_2Hb and Hbdiff are comparable to PO_2.

One NIRS parameter that was particularly interesting was Hbdiff, the calculated difference between O_2Hb and HHb. Hbdiff reflects the oxygenation status of the tissue. For example, when O_2Hb increases, HHb decreases, and therefore the difference between the two parameters increases. Conversely, as the O_2Hb decreases, the HHb increases, and the difference between the two measures decreases. In this 7-day experiment, we observed that Hbdiff increased and decreased with the induced MAP increases and decreases on the day of surgery (Day 1; $n=6$), 2 days post-injury (Day 3; $n=5$), and 7 days post-injury (Day 8; $n=5$), and was typically more sensitive to changes in MAP than to the IP measure of PO_2 (Fig. 7).

Discussion

Hemodynamic management is one of the only treatment options currently available for individuals who suffer an acute SCI. For frontline providers, aggressive augmentation of a patient's MAP is a readily achievable therapeutic approach with the potential to mediate ischemia and maximize tissue sparing in the injured spinal cord. Current clinical guidelines for acute SCI patients recommend increasing MAP to 85–90 mm Hg for 7 days post-injury to maintain adequate perfusion during the acute injury period.[7] However, the evidence supporting specific MAP target values is weak, with conflicting reports on whether they improve neurological outcome.[14,43–46] In a study examining spinal cord perfusion pressure (SCPP), different MAP levels were required to reach the reported optimal SCPP value (where SCPP is the difference between MAP and intrathecal pressure), suggesting that specific MAP targets may be beneficial for some patients, but could be harmful for others.[47] Therefore, optimizing hemodynamic management of acute SCI is paramount and without a method to monitor the physiological response in the injured cord to these hemodynamic alterations, achieving such individual optimization is unlikely.

To attempt to bridge this gap, we developed a sensor using NIRS to provide real-time information about oxygenation and hemodynamics in the injured spinal cord. We previously demonstrated the feasibility and validity of our customized NIRS sensor in an ''ideal'' setting of an anesthetized non-survival large-animal model of SCI to monitor such physiological changes, which yielded a high degree of sensitivity and specificity in detecting spinal cord

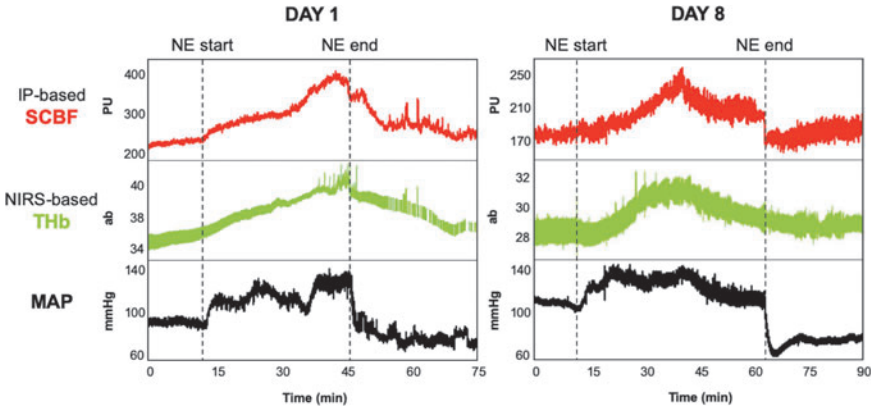

FIG. 5. MAP increase by 20 mm Hg using (NE). Increasing the MAP on Day 1 results in an increase in SCBF measured with the IP sensor, which is mirrored by an increase in the NIRS THb measurement. Both responses are maintained on Day 8 in the same animal. IP, intraparenchymal; MAP, mean arterial blood pressure; NE, norepinephrine; NIRS, near-infrared spectroscopy; SCBF, spinal cord blood flow; THb, total hemoglobin. Color image is available online.

Table 2. Pearson Correlation Coefficients

Relationship between NIRS and IP measures

Measure	*Measure*	*Pearson correlation coefficient*	P-*value*
NIRS O_2Hb	IP PO_2	0.736	$p<0.0001$
NIRS Hbdiff	IP PO_2	0.717	$p<0.0001$
NIRS TOI	IP PO_2	0.613	$p<0.0001$
NIRS THb	IP SCBF	0.492	$p<0.001$

Relationship between NIRS and MAP measures

Measure	*Measure*	*Pearson Correlation Coefficient*	P-*value*
NIRS O_2Hb	MAP	0.715	$p<0.0001$
NIRS Hbdiff	MAP	0.653	$p<0.001$
NIRS TOI	MAP	0.434	$p<0.05$
NIRS THb	MAP	0.718	$p<0.0001$

Based on the correlation coefficients and *p*-values, the correlation relationships of the NIRS measures with each of IP and MAP are statistically significant.

Hbdiff, oxygenated-deoxygenated hemoglobin difference; IP, intraparenchymal; MAP, mean arterial blood pressure; NIRS, near-infrared spectroscopy; O_2Hb, oxygenated hemoglobin; PO_2, partial pressure of oxygen; SCBF, spinal cord blood flow; THb, total hemoglobin; TOI, tissue oxygenation index.

oxygenation changes.[16] In this present study, we confirm that this monitoring could be extended for 7 days in the same animal model, as this is the time window recommended by current clinical guidelines for MAP augmentation.[7]

NIRS-derived measures of oxygenation and hemodynamics were monitored successfully during episodes of ventilatory hypoxia and alterations of MAP throughout the 7-day post-operative period. We assessed how well the minimally invasive NIRS and invasive IP oxygenation measures correlate, given that each of them measures tissue oxygenation status in the spinal cord using slightly different parameters. IP-derived PO_2 provides a measure of the local PO_2 dissolved within the tissue,[48] whereas NIRS-derived O_2Hb and the calculated value, Hbdiff, provide measures of the concentration of oxygen-carrying hemoglobin and represent regional tissue oxygen demand, supply, and utilization.[49] We compared PO_2 with O_2Hb and with Hbdiff, as both are validated indices of local tissue oxygenation.[49,50] In addition, we recognize that IP-derived SCBF reflects temporal changes of blood flow, whereas NIRS-derived THb represents changes of local blood volume in the spinal cord tissue.[29,30] Although THb and SCBF represent different aspects of microcirculatory hemodynamics, similar patterns of change are observed in each of the measurements in response to increases in MAP, indicating an overall increased hemodynamic response in the injured cord.

The observation that the minimally invasive NIRS measures statistically significantly correlate with the invasive IP measures is important from a translational perspective. In its ultimate application for human SCI, such invasive IP measurements will not be available for comparison, because the invasive IP probes in this experiment were only used to validate the NIRS measurements. In terms of clinical applications, our results indicate that the NIRS sensor is able to provide measurements of what is indeed occurring within the injured spinal cord in response to alterations in the MAP. The NIRS measures are also strongly related to the invasive MAP measurements, demonstrating that the NIRS sensor is able to detect local tissue changes within the injured spinal cord that reflect systemic hemodynamic changes (MAP) over the first 7 days post-injury.

The Bland-Altman plots also reveal that the calculated differences between the NIRS measurements of O_2Hb and Hbdiff compared with the IP measurement of PO_2 are in agreement and these parameters may therefore be used comparably in a clinical context.[42,51]

Monitoring tissue oxygenation is already an established approach in the management of traumatic brain injury (TBI) to minimize secondary hypoxic and ischemic brain damage.[52] Several studies have demonstrated the importance of monitoring brain oxygenation to guide clinical decisions and improve diagnoses.[53–55] In patients with severe TBI, care driven by brain tissue oxygenation monitoring resulted in improved clinical outcomes and significantly reduced mortality rates.[54,55] This emphasizes the importance of ensuring oxygen supply to compromised neural tissue and the relevance of translating the principles of this clinical TBI management approach into a strategy for optimized oxygen delivery and hemodynamic management in patients with acute SCI.

We recognize that this study has limitations. The NIRS sensor was positioned rostral to the injury site, whereas the IP probes were inserted caudal to the injury. Although both the NIRS sensor and IP probes were measuring 3.5 cm away from the injury site, it is possible that the sensors were monitoring different responses from

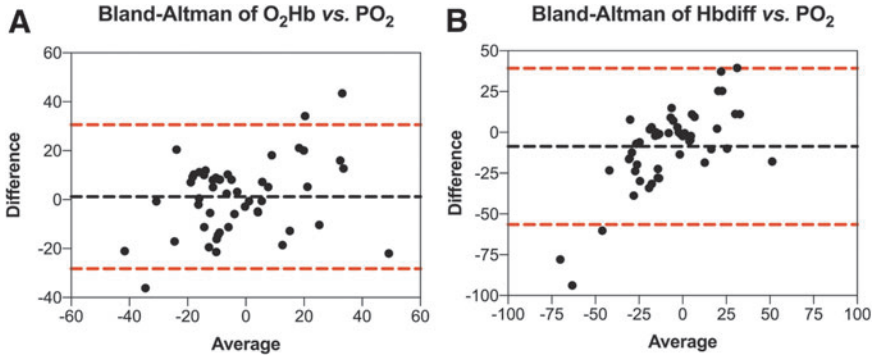

FIG. 6. Bland-Altman plots comparing NIRS **(A)** O_2Hb and **(B)** Hbdiff to IP PO_2. The differences between the NIRS and IP measurements are plotted against the averages of the two measurements. The dotted horizontal black line represents the mean differences between the two methods. The dotted horizontal red line represents the upper and lower 95% limits of agreement (mean difference $\pm 1.96 \times$ SD). IP, intraparenchymal; NIRS, near-infrared spectroscopy; SD, standard deviation. Color image is available online.

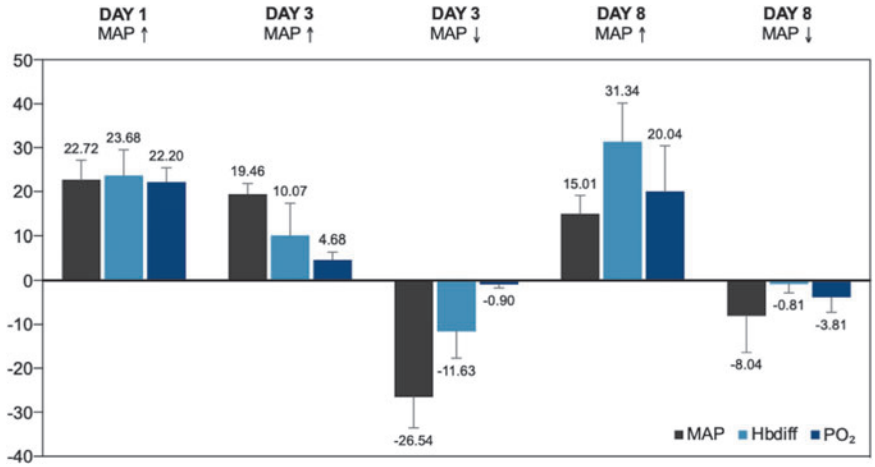

FIG. 7. Oxygenation measurements during MAP alterations. The relationship between non-invasive NIRS Hbdiff and invasive IP PO_2 during induced MAP changes on the day of surgery (Day 1), 2 days post-injury (Day 3), and 7 days post-injury (Day 8). Data are presented as mean ± SEM. Hbdiff, oxygenated-deoxygenated hemoglobin difference; IP, intraparenchymal; MAP, mean arterial blood pressure; NIRS, near-infrared spectroscopy; PO_2, partial pressure of oxygen; SEM, standard error of the mean. Color image is available online.

either side of the injured spinal cord tissue. Despite the different locations, previous studies have reported similar changes in SCBF rostral and caudal to the site of injury in both a rat and rhesus monkey model of SCI, which should be expected given the segmental blood supply to the spinal cord.[56,57] In addition, placement of the NIRS and IP sensors 3.5 cm away from the epicenter of injury likely resulted in measurements from relatively normal spinal cord tissue,[33] and may not be representative of measurements from the injured spinal cord tissue. However, due to the experimental setup for injury and positioning of the impactor, the NIRS sensor was already placed as close to the site of injury as possible, to provide both pre- and post-SCI measurements without disruption of the sensor-dura interface during the actual impact.

We also recognize the limited range of 20 mm Hg for MAP alterations may not fully represent clinical reality, as some patients experience changes in MAP beyond this range.[47] However, because this was a 7-day survival study, we did not want to risk inducing a high range of MAP alterations, and therefore studying the relationship between MAP and NIRS parameters will require further studies. Further, there are occasions where changes in NIRS O_2Hb, Hbdiff, TOI, and THb do not follow the exact changes in MAP. A low Pearson correlation coefficient is observed between the NIRS TOI and MAP measures, suggesting that there are times when the MAP is altered, but the tissue oxygenation remains unchanged. This highlights the importance of being able to know what is happening inside the spinal cord, and not solely inferring physiological responses based on the MAP.

Although the NIRS sensor is able to provide high-frequency data, the NIRS measures are sensitive to movements in the awake animal. On Day 3, monitoring awake and mobile animals resulted in several movement artifacts in both the NIRS and IP measures, although such movements did not change the overall oxygenation and hemodynamic measures. By removing movement artifacts, we are able to mitigate the effects of movement from the NIRS data. The addition of an automatic movement artifact removal filter into the NIRS software algorithm will improve the clinical NIRS system.

This is the first report of maintenance of a fully functioning NIRS sensor directly applied on the dura of the spinal cord for 7 days post-injury. Before advancing to clinical trials, it will be critical to fully investigate the safety of the NIRS sensor, and to establish the potential for the NIR light firing from the sensor to generate heat, or the sensor itself to exert any adverse physical pressure onto the spinal cord. These potential issues will need to be addressed in *in vitro* and *in vivo* studies, as well as through histological examination of the spinal cord tissue at the monitoring site. The NIRS sensor, controller unit, and software will also need further technical refinement before the system is introduced into clinical trials. This will ensure that a safe, biocompatible, and miniaturized device with the smallest possible footprint can be secured on the surface of the dura and be maintained in place for several days of monitoring, followed by easy and safe removal from the patient at the end of the monitoring period.

Overall, this study demonstrates the feasibility of a novel NIRS approach for monitoring changes in spinal cord tissue oxygenation and hemodynamics in a large-animal model for 7 days post-injury. We demonstrated that, during the acute injury period, the NIRS system can detect physiological changes that are strongly associated with changes detected by IP monitoring probes and changes in MAP. Our novel NIRS sensor could ultimately provide clinicians with real-time information about spinal cord physiology, thereby enabling an individualized approach to hemodynamic management. We aim to translate this NIRS system into clinical practice to help clinicians optimize the hemodynamic management of patients with acute SCI and improve the chances of neurological recovery following injury.

Acknowledgments

The authors gratefully acknowledge the technical expertise and contributions of Dr. Behnam Molavi in design and development of the NIRS prototypes. The authors also gratefully acknowledge the staff at the UBC Center for Comparative Medicine (CCM), who support these complex *in vivo* experiments and who provide care for the animals involved in the studies.

Funding Information

This study was supported by a Translational Research Award from the U.S. Department of Defense, Spinal Cord Injury Research Program (SCIRP), SC130007, and an International Collaboration

On Repair Discoveries (ICORD) Seed Grant from the Blusson Integrated Cures Partnership. B.K.K. is the Canada Research Chair in Spinal Cord Injury and the Dvorak Chair in Spine Trauma. B.S. holds a Scholar Award from the Michael Smith Foundation for Health Research.

Author Disclosure Statement

No competing financial interests exist.

References

1. Tator, C.H., and Fehlings, M.G. (1991). Review of the secondary injury theory of acute spinal cord trauma with emphasis on vascular mechanisms. J. Neurosurg. 75, 15–26.
2. Senter, H.J., and Venes, J.L. (1978). Altered blood flow and secondary injury in experimental spinal cord trauma. J. Neurosurg. 49, 569–578.
3. Varma, A.K., Das, A., Wallace, G., Barry, J., Vertegel, A.A., Ray, S.K., and Banik, N.L. (2013). Spinal cord injury: a review of current therapy, future treatments, and basic science frontiers. Neurochem. Res. 38, 895–905.
4. Domingo, A., Al-Yahya, A.A., Asiri, Y., Eng, J.J., and Lam, T. (2012). A systematic review of the effects of pharmacological agents on walking function in people with spinal cord injury. J. Neurotrauma 29, 865–879.
5. Dakson, A., Brandman, D., Thibault-Halman, G., and Christie, S.D. (2017). Optimization of the mean arterial pressure and timing of surgical decompression in traumatic spinal cord injury: a retrospective study. Spinal Cord 55, 1033.
6. Ryken, T.C., Hurlbert, R.J., Hadley, M.N., Aarabi, B., Dhall, S.S., Gelb, D.E., Rozzelle, C.J., Theodore, N., and Walters, B.C. (2013). The acute cardiopulmonary management of patients with cervical spinal cord injuries. Neurosurgery 72, 84–92.
7. Consortium for Spinal Cord Medicine. (2008). Early acute management in adults with spinal cord injury: a clinical practice guideline for health-care professionals. J. Spinal Cord Med. 31, 403–479.
8. Hawryluk, G., Whetstone, W., Saigal, R., Ferguson, A., Talbott, J., Bresnahan, J., Dhall, S., Pan, J., Beattie, M., and Manley, G. (2015). Mean arterial blood pressure correlates with neurological recovery after human spinal cord injury: analysis of high frequency physiologic data. J. Neurotrauma 32, 1958–1967.
9. Catapano, J.S., Hawryluk, G.W.J., Whetstone, W., Saigal, R., Ferguson, A., Talbott, J., Bresnahan, J., Dhall, S., Pan, J., Beattie, M., and Manley, G. (2016). Higher mean arterial pressure values correlate with neurologic improvement in patients with initially complete spinal cord injuries. World Neurosurg. 96, 72–79.
10. Wolf, A., Levi, L., Mirvis, S., Ragheb, J., Huhn, S., Rigamonti, D., and Robinson, W.L. (1991). Operative management of bilateral facet dislocation. J. Neurosurg. 75, 883–890.
11. Vale, F.L., Burns, J., Jackson, A.B., and Hadley, M.N. (1997). Combined medical and surgical treatment after acute spinal cord injury: results of a prospective pilot study to assess the merits of aggressive medical resuscitation and blood pressure management. J. Neurosurg. 87, 239–246.
12. Yue, J.K., Tsolinas, R.E., Burke, J.F., Deng, H., Padhyayula, P.S., Binson, C.K., Lee, Y.M., Han, A.K., Winkler, E.A., and Dhall, S.S. (2019). Vasopressor support in managing acute spinal cord injury: current knowledge. J. Neurosurg. Sci. 63, 308–317.
13. Sabit, B., Zeiler, F.A., and Berrington, N. (2018). The impact of mean arterial pressure on functional outcome post trauma-related acute spinal cord injury: a scoping systematic review of the human literature. J. Intensive Care Med. 33, 3–15.
14. Evaniew, N., Mazlouman, S.J., Belley-Côté, E.P., Jacobs, W.B., and Kwon, B.K. (2019). Interventions to optimize spinal cord perfusion in patients with acute traumatic spinal cord injuries : a systematic review. J. Neurotrauma 37, 1127–1139.
15. Gallagher, M.J., Hogg, F.R.A., Zoumprouli, A., Papadopoulos, M.C., and Saadoun, S. (2019). Spinal cord blood flow in patients with acute spinal cord injuries. J. Neurotrauma 36, 919–929.
16. Shadgan, B., Macnab, A., Fong, A., Manouchehri, N., So, K., Shortt, K., Streijger, F., Cripton, P.A., Sayre, E.C., Dumont, G.A., Pagano, R., Kim, K.-T., and Kwon, B.K. (2019). Optical assessment of spinal cord tissue oxygenation using a miniaturized near infrared spectroscopy sensor. J. Neurotrauma 36, 3034–3043.
17. Macnab, A.J., Gagnon, R.E., Gagnon, F.A., and LeBlanc, J.G. (2003). NIRS monitoring of brain and spinal cord—detection of adverse intraoperative events. J. Spectrosc. 17, 483–490.
18. Hamaoka, T., McCully, K.K., Niwayama, M., and Chance, B. (2011). The use of muscle near-infrared spectroscopy in sport, health and medical sciences: recent developments. Philos. Trans. R. Soc. A Math. Phys. Eng. Sci. 369, 4591–4604.
19. Costes, F., Prieur, F., Féasson, L., Geyssant, A., Barthélémy, J.C., and Denis, C. (2001). Influence of training on NIRS muscle oxygen saturation during submaximal exercise. Med. Sci. Sports Exerc. 33, 1484–1489.
20. McCormick, P.W., Stewart, M., Goetting, M.G., Dujovny, M., Lewis, G., and Ausman, J.I. (1991). Noninvasive cerebral optical spectroscopy for monitoring cerebral oxygen delivery and hemodynamics. Crit. Care Med. 19, 89–97.
21. Jobsis, F. (1977). Noninvasive, infrared monitoring of cerebral and myocardial oxygen sufficiency and circulatory parameters. Science. 198, 1264–1267.
22. Delpy, D.T., Cope, M., Van Der Zee, P., Arridge, S., Wray, S., and Wyatt, J. (1988). Estimation of optical pathlength through tissue from direct time of flight measurement. Phys. Med. Biol. 33, 1433–1442.
23. Boushel, R., Langberg, H., Olesen, J., Nowak, M., Simonsen, L., Bulow, J., and Kjaer, M. (2000). Regional blood flow during exercise in humans measured by near-infrared spectroscopy and indocyanine green. J. Appl. Physiol. 89, 1868–1878.
24. Mancini, D.M., Bolinger, L., Li, H., Kendrick, K., Chance, B., and Wilson, J.R. (1994). Validation of near-infrared spectroscopy in humans. J. Appl. Physiol. 77, 2740–2747.
25. Matcher, S.J., Elwell, C.E., Cooper, C.E., Cope, M., and Delpy, D.T. (1995). Performance comparison of several published tissue near-infrared spectroscopy algorithms. Anal. Biochem. 227, 54–68.
26. Ferraris, A., Jacquet-Lagrèze, M., and Fellahi, J.L. (2018). Four-wavelength near-infrared peripheral oximetry in cardiac surgery patients: a comparison between EQUANOX and O3. J. Clin. Monit. Comput. 32, 253–259.
27. Wyser, D., Lambercy, O., Scholkmann, F., Wolf, M., and Gassert, R. (2017). Wearable and modular functional near-infrared spectroscopy instrument with multidistance measurements at four wavelengths. Neurophotonics 4, 041413.
28. Tachtsidis, I., Tisdall, M.M., Leung, T.S., Pritchard, C., Cooper, C.E., Smith, M., and Elwell, C.E. (2009). Relationship between brain tissue haemodynamics, oxygenation and metabolism in the healthy human adult brain during hyperoxia and hypercapnea. Adv. Exp. Med. Biol. 645, 315–320.
29. Ferrari, M., Muthalib, M., and Quaresima, V. (2011). The use of near-infrared spectroscopy in understanding skeletal muscle physiology: recent developments. Philos. Trans. R. Soc. A Math. Phys. Eng. Sci. 369, 4577–4590.
30. Macnab, A., and Shadgan, B. (2012). Biomedical applications of wireless continuous wave near infrared spectroscopy. Biomed. Spectrosc. Imaging 1, 205–222.
31. Hagino, I., Anttila, V., Zurakowski, D., Duebener, L.F., Lidov, H.G.W., and Jonas, R.A. (2005). Tissue oxygenation index is a useful monitor of histologic and neurologic outcome after cardiopulmonary bypass in piglets. J. Thorac. Cardiovasc. Surg. 130, 384–392.
32. Kovacsova, Z., Bale, G., Mitra, S., de Roever, I., Meek, J., Robertson, N., and Tachtsidis, I. (2018). Investigation of confounding factors in measuring tissue saturation with NIRS spatially resolved spectroscopy. Adv. Exp. Med. Biol. 1072, 307–312.
33. Streijger, F., So, K., Manouchehri, N., Tigchelaar, S., Lee, J.H.T., Okon, E.B., Shortt, K., Kim, S.-E., McInnes, K., Cripton, P., and Kwon, B.K. (2017). Changes in pressure, hemodynamics, and metabolism within the spinal cord during the first 7 days after injury using a porcine model. J. Neurotrauma 34, 3336–3350.
34. Kim, K.T., Streijger, F., So, K., Manouchehri, N., Shortt, K., Okon, E.B., Tigchelaar, S., Fong, A., Morrison, C., Keung, M., Sun, J., Liu, E., Cripton, P.A., and Kwon, B.K. (2019). Differences in morphometric measures of the uninjured porcine spinal cord and dural sac predict histological and behavioral outcomes after traumatic spinal cord injury. J. Neurotrauma 36, 3005–3017.
35. Micheels, J., Aisbjorn, B., and Sorensen, B. (1984). Laser doppler flowmetry. a new non-invasive measurement of microcirculation in intensive care? Resuscitation 12, 31–39.
36. Griffiths, J.R., and Robinson, S.P. (1999). The OxyLite: a fibre-optic oxygen sensor. Br. J. Radiol. 72, 627–630.

37. Roriz, P., Frazão, O., Lobo-Ribeiro, A.B., Santos, J.L., and Simões, J.A. (2013). Review of fiber-optic pressure sensors for biomedical and biomechanical applications. J. Biomed. Opt. 18, 050903.
38. Poeggel, S., Tosi, D., Duraibabu, D., Leen, G., McGrath, D., and Lewis, E. (2015). Optical fibre pressure sensors in medical applications. Sensors 15, 17115–17148.
39. Streijger, F., So, K., Manouchehri, N., Gheorghe, A., Okon, E.B., Chan, R.M., Ng, B., Shortt, K., Sekhon, M.S., Griesdale, D.E., and Kwon, B.K. (2018). A direct comparison between norepinephrine and phenylephrine for augmenting spinal cord perfusion in a porcine model of spinal cord injury. J. Neurotrauma 35, 1345–1357.
40. Cheung, A., Streijger, F., So, K., Okon, E.B., Manouchehri, N., Shortt, K., Kim, K.-T., Keung, M.S.M., Chan, R.M., Fong, A., Sun, J., Griesdale, D.E., Sehkon, M.S., and Kwon, B.K. (2020). Relationship between early vasopressor administration and spinal cord hemorrhage in a porcine model of acute traumatic spinal cord injury. J. Neurotrauma 37, 1–12.
41. Bland, J.M., and Altman, D.G. (2007). Agreement between methods of measurement with multiple observations per individual. J. Biopharm. Stat. 17, 571–582.
42. Martin Bland, J., and Altman, D.G. (1986). Statistical methods for assessing agreement between two methods of clinical measurement. Lancet 47, 931–936.
43. Cohn, J., Wright, J., McKenna, S., and Bushnik, T. (2010). Impact of mean arterial blood pressure during the first seven days post spinal cord injury. Top. Spinal Cord Inj. Rehabil. 15, 96–106.
44. Inoue, T., Manley, G.T., Patel, N., and Whetstone, W.D. (2014). Medical and surgical management after spinal cord injury: vasopressor usage, early surgerys, and complications. J. Neurotrauma 31, 284–291.
45. Kepler, C.K., Schroeder, G.D., Martin, N.D., Vaccaro, A.R., Cohen, M., and Weinstein, M.S. (2015). The effect of preexisting hypertension on early neurologic results of patients with an acute spinal cord injury. Spinal Cord 53, 763.
46. Martin, N.D., Kepler, C., Zubair, M., Sayadipour, A., Cohen, M., and Weinstein, M. (2015). Increased mean arterial pressure goals after spinal cord injury and functional outcome. J. Emerg. Trauma. Shock 8, 94.
47. Kong, C.Y., Hosseini, A.M., Belanger, L.M., Ronco, J.J., Paquette, S.J., Boyd, M.C., Dea, N., Street, J., Fisher, C.G., Dvorak, M.F., and Kwon, B.K. (2013). A prospective evaluation of hemodynamic management in acute spinal cord injury patients. Spinal Cord 51, 466–471.
48. Ma, Y., and Wu, S. (2008). Simultaneous measurement of brain tissue oxygen partial pressure, temperature, and global oxygen consumption during hibernation, arousal, and euthermy in non-sedated and non-anesthetized Arctic ground squirrels. J. Neurosci. Methods 174, 237–244.
49. Ferrari, M., Mottola, L., and Quaresima, V. (2004). Principles, techniques, and limitations of near infrared spectroscopy. Can. J. Appl. Physiol. 29, 463–487.
50. Ortiz-Prado, E., Dunn, J.F., Vasconez, J., Castillo, D., and Viscor, G. (2019). Partial pressure of oxygen in the human body: a general review. Am. J. Blood Res. 9, 1–14.
51. Stöckl, D., Rodríguez Cabaleiro, D., Van Uytfanghe, K., and Thienpont, L.M. (2004). Interpreting method comparison studies by use of the Bland-Altman plot: reflecting the importance of sample size by incorporating confidence limits and predefined error limits in the graphic. Clin. Chem. 50, 2216–2218.
52. Bratton, S., Chestnut, R., Ghajar, J., McConnell Hammond, F., Harris, O., Hartl, R., Manley, G., Nemecek, A., Newell, D., Rosenthal, G., Schouten, J., Shutter, L., Timmons, S., Ullman, J., Videtta, W., Wilberger, J., and Wright, D. (2007). Guidelines for the management of severe traumatic brain injury. X. Brain oxygen monitoring and thresholds. J. Neurotrauma 24, Suppl. 1, S65–S70.
53. Kiening, K.L., Unterberg, A.W., Bardt, T.F., Schneider, G.H., and Lanksch, W.R. (1996). Monitoring of cerebral oxygenation in patients with severe head injuries: brain tissue PO2 versus jugular vein oxygen saturation. J. Neurosurg. 85, 751–757.
54. Pascual, J.L., Georgoff, P., Maloney-Wilensky, E., Sims, C., Sarani, B., Stiefel, M.F., Leroux, P.D., and Schwab, C.W. (2011). Reduced brain tissue oxygen in traumatic brain injury: are most commonly used interventions successful? J. Trauma 70, 535–546.
55. Stiefel, M.F., Spiotta, A., Gracias, V.H., Garuffe, A.M., Guillamondegui, O., Maloney-Wilensky, E., Bloom, S., Grady, M.S., and LeRoux, P.D. (2005). Reduced mortality rate in patients with severe traumatic brain injury treated with brain tissue oxygen monitoring. J. Neurosurg. 103, 805–811.
56. Kawata, K., Morimoto, T., Ohashi, T., Tsujimoto, S., Hoshida, T., Tsunoda, S., and Sakaki, T. (1993). Experimental study of acute spinal cord injury: a study of spinal blood flow. Neurol. Surg. 21, 239–245.
57. Kobrine, A.I., Doyle, T.F., and Martins, A.N. (1975). Local spinal cord blood flow in experimental traumatic myelopathy. J. Neurosurg. 42, 144–149.

Address correspondence to:
Babak Shadgan, MD, MSc, PhD
Department of Orthopedics
University of British Columbia
5440, Blusson Spinal Cord Center
Vancouver General Hospital
818 West 10th Avenue
Vancouver, British Columbia V5Z 1M9
Canada

E-mail: shadgan@mail.ubc.ca